Fgf3 signaling from the ventral diencephalon is required for early specification and subsequent survival of the zebrafish adenohypophysis

Wiebke Herzog[1,*], Carmen Sonntag[1], Sophia von der Hardt[1], Henry H. Roehl[2,†], Zoltan M. Varga[3] and Matthias Hammerschmidt[1,‡]

[1]Max-Planck Institute for Immunobiology, Stuebeweg 51, 79108 Freiburg, Germany
[2]Max-Planck Institute for Developmental Biology, Spemannstraße 35, 72076 Tübingen, Germany
[3]University of Freiburg, Department of Biology I, Hauptstraße 1, 79104 Freiburg, Germany
*Present address: Programs in Developmental Biology and Human Genetics, Department of Biochemistry and Biophysics, UCSF, San Fransisco, CA 94143-0448, USA
†Present address: University of Sheffield, Department of Biomedical Science, Firth Court, Western Bank, Sheffield S10 2TN, UK
‡Author for correspondence (e-mail: hammerschmid@immunbio.mpg.de)

Accepted 21 April 2004

Development 131, 3681-3692
Published by The Company of Biologists 2004
doi:10.1242/dev.01235

Summary

The pituitary gland consists of two major parts: the neurohypophysis, which is of neural origin; and the adenohypophysis, which is of non-neural ectodermal origin. Development of the adenohypophysis is governed by signaling proteins from the infundibulum, a ventral structure of the diencephalon that gives rise to the neurohypophysis. In mouse, the fibroblast growth factors Fgf8, Fgf10 and Fgf18 are thought to affect multiple processes of pituitary development: morphogenesis and patterning of the adenohypophyseal anlage; and survival, proliferation and differential specification of adenohypophyseal progenitor cells. Here, we investigate the role of Fgf3 during pituitary development in the zebrafish, analyzing *lia*/*fgf3* null mutants. We show that Fgf3 signaling from the ventral diencephalon is required in a non-cell autonomous fashion to induce the expression of *lim3*, *pit1* and other pituitary-specific genes in the underlying adenohypophyseal progenitor cells. Despite the absence of such early specification steps, *fgf3* mutants continue to form a distinct pituitary anlage of normal size and shape, until adenohypophyseal cells die by apoptosis. We further show that Sonic Hedgehog (Shh) cannot rescue pituitary development, although it is able to induce adenohypophyseal cells in ectopic placodal regions of *fgf3* mutants, indicating that Fgf3 does not act via Shh, and that Shh can act independently of Fgf3. In sum, our data suggest that Fgf3 signaling primarily promotes the transcriptional activation of genes regulating early specification steps of adenohypophyseal progenitor cells. This early specification seems to be essential for the subsequent survival of pituitary cells, but not for pituitary morphogenesis or pituitary cell proliferation.

Key words: Fgf3, Pituitary, Adenohypophysis, Neurohypophysis, Zebrafish, Lia, Cell survival, Cell specification, Apoptosis, Sonic Hedgehog

Introduction

The pituitary gland links the nervous system with the endocrine system of vertebrates, responding to signals from the hypothalamus with the production and release of peptide hormones that regulate vital processes in metabolism, reproduction and growth. It consists of two parts that both secrete hormones: the posterior pituitary, also called the neurohypophysis, and the anterior pituitary, called the adenohypophysis. Neurohypophyseal hormones are generated in neuroendocrine cells in the hypothalamus, from where they are brought to the neurohypophysis via axonal transport, whereas adenohypophyseal hormones are generated in pituitary cells themselves. In mammals, these can be subdivided into different cell types, characterized by the hormones they produce: lactotropes producing prolactin (Prl), somatotropes producing growth hormone (Gh), thyrotropes producing thyroid-stimulating hormone (Tsh), gonadotropes producing luteinizing or follicle-stimulating hormone (Lh, Fsh), and corticotropes and melanotropes producing a common precursor peptide, Proopiomelanocortin (Pomc), which is proteolytically cleaved to give rise to adrenocorticotropin (Acth) and melanocyte-stimulating hormone (Msh).

The neurohypophysis is of neuroectodermal origin and derives from the infundibulum, an evagination of the ventral diencephalon. By contrast, the adenohypophysis is a derivative of the non-neuronal, placodal ectoderm. It is initially located at the anterior neural ridge (ANR) and becomes part of the oral roof ectoderm, from where it invaginates toward the presumptive neurohypophysis/infundibulum, forming Rathke's pouch. This co-development of neuro- and adenohypophysis is governed by various signaling processes between infundibulum and adenohypophyseal placode (for reviews, see Treier and Rosenfeld, 1996; Burgess et al., 2002; Scully and Rosenfeld, 2002). For example, the infundibulum generates at least three members of the fibroblast growth factor (Fgf) family, Fgf8,

Fgf10 and Fgf18 (Norlin et al., 2000; Ohuchi et al., 2000). Gain-of-function studies with *fgf8* transgenic mice or pituitary explants treated with Fgf8 beads suggest that Fgf signaling promotes the proliferation and differentiation of dorsal cell types of the adenohypophysis (corticotropes and melanotropes), antagonized by Bmp2, which promotes ventral cell fates (thyrotropes, gonadotropes, somatotropes and lactotropes) (Ericson et al., 1998; Treier et al., 1998). Consistent results were obtained in loss-of-function studies, showing that treatment of embryonic day (E) 10 pituitary transplants with the Fgf receptor inhibitor SU5402 (Mohammadi et al., 1997) selectively blocks the proliferation and generation of dorsal cell types (Norlin et al., 2000). Together, the data suggest a patterning and cell type selective role for Fgf signaling. By contrast, knockout mice deficient in Fgf10 (Ohuchi et al., 2000) or the Fgf receptor 2 isoform IIIB (Fgfr2IIIb) (De Moerlooze et al., 2000) display a poorly formed Rathke's pouch, with numerous apoptotic cells throughout the entire pouch. These defects are already apparent at E10, suggesting an earlier and more general role for Fgf signaling during mouse pituitary development, affecting pouch morphogenesis and the survival and proliferation of all adenohypophyseal progenitor cells.

Here, we describe mutant analyses to uncover the role of Fgf3 during adenohypophysis development in the zebrafish. Recent work has revealed both striking similarities and differences in pituitary development between the different vertebrate classes. Thus, we found that despite differences in the morphogenesis and architecture of their pituitary glands, the role of Sonic Hedgehog during induction, growth and patterning of the adenohypophyseal anlage appears to be largely conserved between zebrafish and mouse (Herzog et al., 2003; Sbrogna et al., 2003). To isolate additional genes required for zebrafish pituitary development, we conducted a screen for ENU-induced mutations affecting adenohypophyseal production of Gh (Herzog et al., 2004). One gene identified in this screen is the pituitary-specific transcription factor Pit1. *pit1* mutant zebrafish are semi-viable and show very similar phenotypic traits to those of their human and mouse counterparts (Nica et al., 2004), strengthening the value of the zebrafish system as a clinically relevant model organism. Here, we show that another identified gene, *lim-absent* (*lia*), encodes zebrafish Fgf3 (Kiefer et al., 1996). Using antisense-mediated inactivation, *fgf3* has recently been proposed to be necessary for craniofacial development (David et al., 2002; Walshe and Mason, 2003b) and, in partial redundancy with *fgf8*, telencephalic patterning (Shanmugalingam et al., 2000; Fürthauer et al., 2001; Shinya et al., 2001; Walshe and Mason, 2003a), hindbrain patterning (Liu et al., 2003a; Maves et al., 2002; Walshe et al., 2002) and otic placode induction (Phillips et al., 2001; Leger and Brand, 2002; Maroon et al., 2002; Liu et al., 2003a). Our mutant analyses confirm most, but not all, of the proposed Fgf3-unique roles.

During pituitary development, Fgf3 is primarily required to promote early specification steps and the subsequent survival of adenohypophyseal cells. However, we find that morphogenesis and growth of the pituitary anlage do not depend upon Fgf3. In addition, we show that the source of Fgf3 is cells of the ventral diencephalon, presumably encompassing the presumptive neurohypophysis.

Materials and methods

Linkage analysis, identification of mutations, and genotyping

Mapping of the *lia*^{t24147} and *lia*^{t24152} mutations was done via PCR analysis of genomic DNA from individual *lia* mutant embryos, as described (Geisler, 2002). For identification of point mutations, *fgf3* cDNA was amplified via RT-PCR, as described (Nica et al., 2004), using the following PCR conditions: 3 minutes at 94°C – 32× (30 seconds at 94°C, 30 seconds at 60°C, 1.5 minutes at 72°C) – 10 minutes at 72°C; sense primer 5′ GCTTGGAGAGCAGAGTGGAAC; antisense primer 5′ GCCTGGGATCTCCATCTGTGTC. In two alleles, the mutations generate restriction length polymorphisms (RFLP), which were used to genotype single embryos via PCR of genomic DNA. For the *fgf3*^{t26212} allele, PCR conditions were: 2 minutes at 94°C – 34× (30 seconds at 94°C, 30 seconds at 58°C, 1 minute at 72°C) – 5 minutes at 72°C; sense primer, 5′ TTCTGCTCTTGTTGTTACTGAGC, antisense primer 5′ TACGCAAGTCCCATGAACTCATC. The obtained 330 bp PCR fragment was digested with *Tsp509*I, leading to a cleavage of the wild-type fragment to a 120 bp fragment and a 210 bp fragment, while the mutant fragment remained at 330 bp. For the *fgf3*^{t24149} allele, PCR conditions were: 2 minutes at 94°C – 35× (30 seconds at 94°C, 30 seconds at 58°C, 1 minute at 72°C) – 5 minutes at 72°C; sense primer 5′ GTCTTCAACCGAGAGTGTG; antisense primer 5′ CTATGCCGGACCCTGTTG. The PCR products were digested with *Hpy188*I, yielding mutant fragments of 90 bp and 20 bp, while the wild-type fragment remained at 110 bp.

Generation of constructs, mRNA synthesis and microinjection

For expression constructs, full-length wild-type and mutant *fgf3* cDNAs were amplified via RT-PCR with primers containing *Eco*RI and *Xba*I restriction sites, and cloned into pCS2+ (Rupp et al., 1994). Capped RNA was prepared with the Message Machine kit (Ambion). *shh* RNA was prepared, and RNA was injected as described (Herzog et al., 2003).

In-situ hybridization, Alcian Blue stainings, Acridine Orange stainings

Whole-mount in-situ hybridizations were carried out as previously described (Hammerschmidt et al., 1996; Herzog et al., 2003). For *fgf3* in-situ probe synthesis, plasmid *pCRII-fgf3* was linearized with *Kpn*I and transcribed with T7 RNA polymerase. In addition, riboprobes of the following cDNAs were used: *dlx2*, *dlx3* (Akimenko et al., 1994), *eya1* (Sahly et al., 1999), *emx1* (Morita et al., 1995), *gh*, *pomc*, *prl* (Herzog et al., 2003), *hgg* (Thisse et al., 1994), *krox20* (Oxtoby and Jowett, 1993), *lim3* (Glasgow et al., 1997), *nkx2.1a* (Rohr and Concha, 2000), *pit1* (Nica et al., 2004), *shh* (Krauss et al., 1993), *spry4* (Fürthauer et al., 2001).

To visualize craniofacial cartilage, 120 hours postfertilization (hpf) embryos were stained with Alcian Blue (Sigma) as described (Schilling et al., 1996).

For detection of apoptotic cells, dechorionated live embryos were incubated for 10 minutes in 5 μg/ml Acridine Orange (Sigma) in embryo medium (E3), followed by fluorescent microscopy (Zeiss axiophot) and photography.

Single cell tracing experiments

To study the fate of pituitary precursor cells, single cells in the prospective pituitary forming region were injected in tailbud-stage embryos with 3% rhodamine dextran (3 kD) in 0.2 M KCl, using an AM-Systems 1600 Neuroprobe amplifier, and the underlying mesodermal polster as a morphological landmark (Varga et al., 1999) (S. Dutta and Z.M.V., unpublished). Fates of labeled daughter cells were analyzed between 24 and 30 hpf, using conventional fluorescence microscopy, or a Zeiss LSM 510 confocal microscope. Individual embryos were genotyped after photography.

SU5402 treatment

Embryos were incubated at 28.5°C in 12 or 20 μM SU5402 containing E3, prepared from a 3 mM SU5402 (Calbiochem, S72630) stock solution in DMSO. Control embryos were incubated in E3 medium with the corresponding amount of DMSO. After treatment, embryos were washed five times with E3/DMSO and transferred to fresh E3.

Cell transplantations

For transplanting wild-type cells into offspring of heterozygous mutants, wild-type embryos were injected with a 1% biotin-dextrane, 0.5% fluorescein dextrane solution. Homotopic transplantations of presumptive telencephalic or diencephalic cells were carried out at the shield stage. At 32 hpf, chimeras were fixed and analyzed by in-situ hybridization, followed by anti-biotin stainings with the Vectastain Elite ABC kit (Vector Laboratories) to stain transplanted cells. The tails of chimeras (containing only recipient-derived cells) were genotyped, as described above.

Bead implantations

Heparin-coated acrylic beads (Sigma, H-5263) were washed twice in PBS, and incubated with 0.5 μg/μl recombinant human FGF3 (R&D Systems, 1206-FG) or 0.5 μg/μl BSA overnight at 4°C. At 19 hpf, offspring from a cross of two t24149/+ carriers were dechorionated, embedded in 1% low melting agarose on agarose-coated petri dishes, and covered with Ringer's solution. Using a fine tungsten needle and forceps, a bead was implanted behind the eye and pushed to the front of the head. After implantation, embryos were left on the plates for recovery for 2 hours at 28.5°C, then carefully taken out of the agarose and incubated for another 5 hours until fixation at 26 hpf.

Results

The *lia* locus encodes zebrafish Fgf3

During a large-scale screen for zebrafish mutants with altered growth hormone expression, we isolated four ENU-induced *lia* mutations. *lia* mutant embryos are characterized by the complete absence of *lim3* expression in the adenohypophyseal anlage at 32 hpf, and the lack of all hormone-producing adenohypophyseal cell types during further development (Herzog et al., 2004). Mutants usually die between 7 and 9 days after fertilization, most likely due to the additional craniofacial defects (see below). Using bulk segregation analysis, *lia* was mapped to linkage group 7. Further fine mapping located *lia* approximately 62 cM from the top of LG7, between the markers Z41496 and Z64508. One of the genes that had previously been mapped to the same region is *fgf3* (wwwmap.tuebingen.mpg.de). Together with the similar craniofacial phenotypes of *lia* mutants and *fgf3* morphants (see below), this made *fgf3* a likely candidate for *lia*.

PCR amplification and sequencing of *fgf3* cDNA from the four different *lia* alleles revealed three missense mutations and one nonsense mutation, leading to exchanges or deletions of highly conserved amino acid residues of Fgf3 protein (Fig. 1A). In the *fgf3*^{t26212} allele, a T-to-A transition leads to the replacement of an isoleucine residue at amino acid position 76 of the protein by an asparagine (I76N). In *fgf3*^{t24149}, a G-to-A transition causes the exchange of glutamate 138 to lysine (E138K). Both mutations generate RFLPs, which were used to confirm the linkage between the *lia* mutations and the *fgf3* gene (no recombination in 436 meioses). In *fgf3*^{t21142}, tyrosine 148 is exchanged to a cysteine (T148C), due to an A-to-G transition, while in the *fgf3*^{t24152} allele, a G-to-A transition introduces a premature stop codon after amino acid residue 177. This results in a deletion of the last 79 amino acids of the protein, including 40 amino acids of the central core of 140 amino acids that is highly conserved among the different Fgf family members (Powers et al., 2000).

All four *lia*/*fgf3* alleles represent strong loss-of-function or null alleles

To determine the effects of the four *lia/fgf3* mutations on the activity of Fgf3 protein, we carried out overexpression studies in zebrafish embryos. Injection of wild-type *fgf3* RNA leads to a general dorsalization of the embryo, and to a posteriorization of its neuroectoderm (Fürthauer et al., 1997; Koshida et al., 2002). For better quantification of these effects, we defined four phenotypic classes of increasing strength, from mild F1 to strong F4 (see legend to Fig. 1B). When injected at a concentration of 0.1 ng/μl, wild-type *fgf3* mRNA was highly effective, whereas all four mutant versions showed hardly any effect (Fig. 1B). Even upon injection at 100-fold higher concentrations (10 ng/μl), *fgf3*^{t24152} and *fgf3*^{t21142} mRNA were ineffective, while *fgf3*^{t26212} and *fgf3*^{t24149} showed some effects that, however, were significantly weaker than those obtained with wild-type mRNA at 0.1 ng/μl (Fig. 1B). Together, these data indicate that the *fgf3*^{t24152} nonsense mutation and the *fgf3*^{t21142} missense mutation are likely to be null mutations (amorphs), while *fgf3*^{t26212} and *fgf3*^{t24149} have retained less than 1% of the normal Fgf3 activity, and can therefore be regarded as very strong hypomorphs or near amorphs. This is consistent with the embryonic defects caused by the *fgf3* mutations, which are of indistinguishable strength for all four alleles.

fgf3 mutants display defects during craniofacial and otic vesicle development

Several recent publications describe *fgf3* and combinatorial *fgf3* and *fgf8* loss-of-function studies, using antisense morpholino oligonucleotide technology (see Introduction). The combinatorial activity of *fgf3* and *fgf8* was reported to be required for otic vesicle formation, telencephalon and hindbrain patterning, and craniofacial development. Most of these processes were also affected upon single loss of *fgf3*; however, the effects were more moderate or more restricted, pointing to partial redundancy of Fgf3 and Fgf8.

During craniofacial development, Fgf3 from the pharyngeal endoderm was reported to be required for the specification and survival of chondrogenic neural crest cells of the gill arches (pharyngeal arches 3-7) (David et al., 2002), while the crest cells forming mandibular and hyoid (pharyngeal arches 1 and 2) are under the redundant control of Fgf3 and Fgf8 (Walshe and Mason, 2003b). Consistent with this notion, Alcian Blue stainings of *fgf3* mutants at 120 hpf revealed an almost complete loss of the cartilage of the gill arches, while the cartilage of mandibular and hyoid was present (Fig. 2G,H). These defects are anticipated by a progressive reduction in the number of *dlx2*-positive chondrogenic neural crest cells of arches 3-7, starting around 26 hpf, while the two anterior *dlx2* domains, forming cartilage of arches 1 and 2, appear normal (Fig. 2C,D). In addition, the posterior *dlx2* domain fails to subdivide into the streams corresponding to the different gill arches (Fig. 2C,D). Similarly, the pharyngeal endoderm remains unsegmented, as reflected by the *fgf3* expression pattern (Fig. 2E,F).

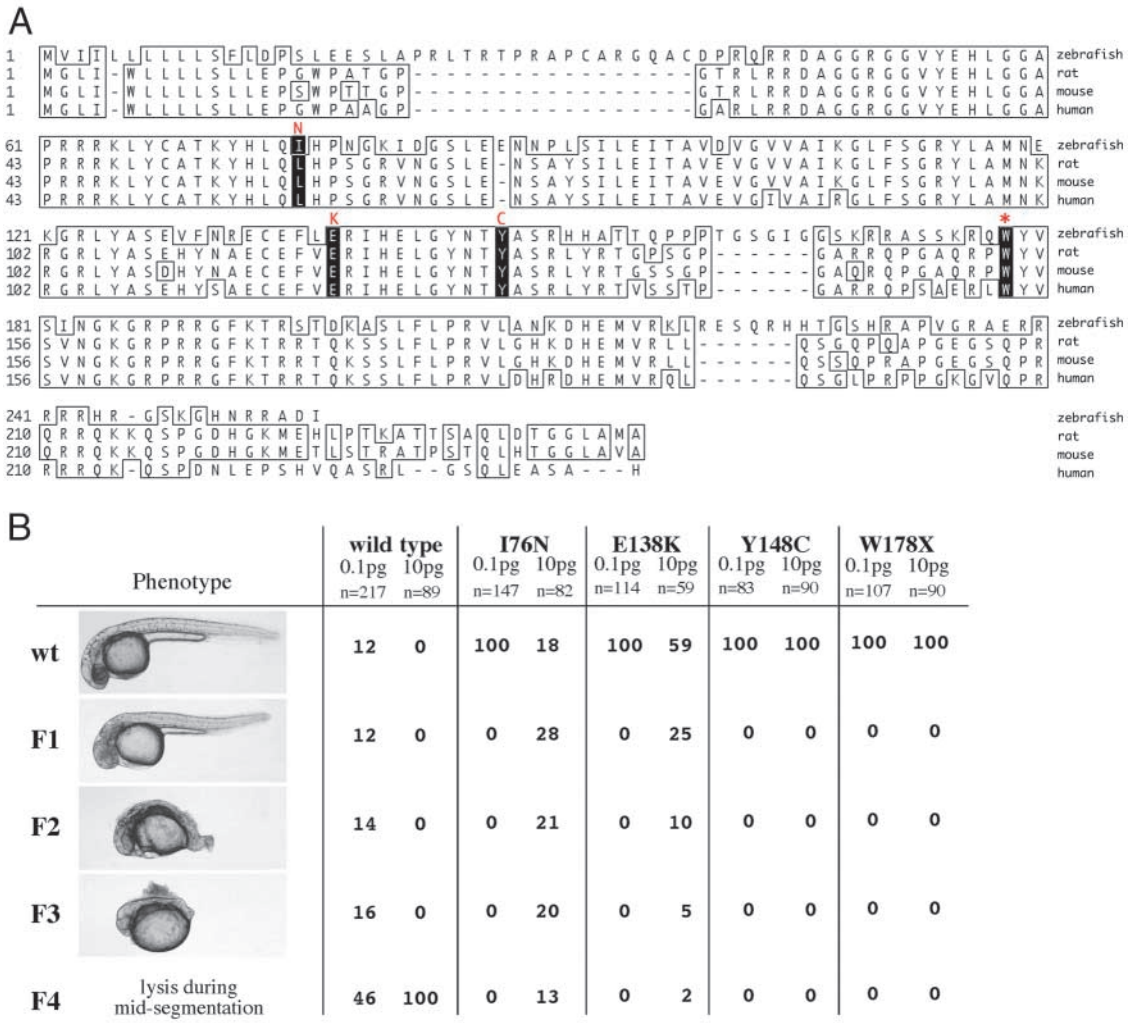

Fig. 1. The four *lia* mutations cause exchanges or deletions of conserved amino acid residues of Fgf3 protein, leading to a complete loss of Fgf3 activity. (A) Amino acid alignment of Fgf3 proteins from zebrafish, rat, mouse and human. Conserved amino acids are boxed, amino acid residues mutated in the different *lia* alleles are highlighted in black, with the new amino acid residues indicated in red. The premature protein termination caused by the *t24152* mutation is indicated with a star (*). (B) Phenotypic classes (F1-F4) and frequencies (%) obtained upon injection of wild-type or mutant *fgf3* mRNAs at concentrations of 0.1 or 10 ng/μl. F1 embryos are characterized by a loss of the eyes and a normal tail; F2 by a loss of eyes, fore- and midbrain, and a curled up, truncated tail; F3 embryos by a complete loss of head and tail; and F4 embryos by lysis around the 10-15 somite stage. Data were obtained in two independent experiments. n, numbers of scored embryos.

We could also confirm the previously reported essential, but partially redundant, role of Fgf3 during inner ear development. Thus, *fgf3* mutants display otic vesicles of reduced size and fused otoliths (Fig. 2G,H). By contrast, mutants show normal expression patterns of *emx1* and *dlx2* in the dorsal and ventral telencephalon (Fig. 2A,B), suggesting that in contrast to a previous report (Walshe et al., 2003a), Fgf3 is dispensable for telencephalic patterning. This discrepancy between mutant and morphant data might be due to toxicity and/or cross-reactions of the *fgf3* morpholino oligonucleotides, possibly with thus far undescribed *fgf*s.

fgf3 expression during adenohypophysis development

By contrast to the processes mentioned above, no role of Fgf3 during adenohypophysis development had been described so far. We carried out double in-situ hybridizations to investigate *fgf3* expression relative to the developing adenohypophysis. At the end of gastrulation (10 hpf), *fgf3* is expressed in the telencephalon, adjacent to the placodal cells of the anterior neural ridge (ANR) that are marked by *dlx3* expression (Fig. 3A). The placodal ectoderm itself is devoid of *fgf3* transcripts. Similarly, the progressing anterior dorsal mesoderm, called polster and marked by the expression of *hgg*, lacks *fgf3* expression (Fig. 3B). Median ventral regions of the neuroectoderm, marked by the expression of *shh* (Fig. 3C) (cf. Varga et al., 1999), might show some weak and diffuse *fgf3* staining (Fig. 3B,E). However, strong and distinct diencephalic *fgf3* expression can first be detected from the 18-somite stage onward (18 hpf), after *fgf3* expression in the telencephalon has ceased (Fig. 3F). Within the diencephalon, *fgf3* expression is restricted to the ventralmost cell layers, as revealed with double-stainings using the hypothalamic marker *nkx2.1a* (Fig. 3I,L). This tuberal region of the posterior-ventral

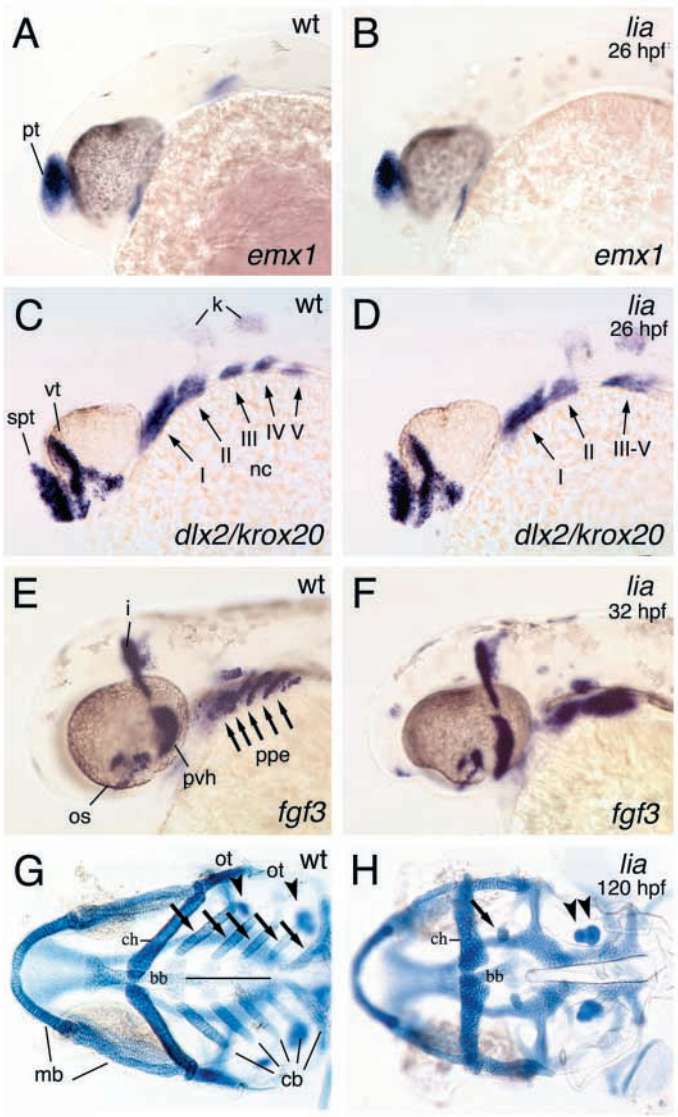

Fig. 2. *fgf3* mutant embryos display defects in otic vesicles, ventral head skeleton and pharyngeal endoderm. Probes used in whole-mount in-situ hybridizations are indicated in the lower right corners, ages of embryos in the upper right corners. Left panels (A,C,E,G) show wild-type siblings (wt), right panels (B,D,F,H) *fgf3* mutants (*lia*). Embryos were genotyped after photography. (A-F) Lateral views. (G,H) Dorsal views on heads. 'k' in C marks *krox20* in rhombomeres 3 and 5. Arrows and numbers in C,D mark neural crest streams to the corresponding pharyngeal arches (I, mandibular; II, hyoid; III, IV, V, gill arches). Arrows in E mark pharyngeal pouches of gill arches. (G,H) Alcian Blue staining of craniofacial cartilage; arrows in G indicate ceratobranchials of the gill arches, arrow in H remaining part of first ceratobranchial of *fgf3* mutant. Arrowheads mark otoliths, which are fused in the mutant. bb, basibranchial; cb, ceratobranchials; ch, ceratohyal; i, isthmus; mb, mandibulare; nc, neural crest; ppe, pharyngeal pouch endoderm; pt, pallial (dorsal) telencephalon; os, optic stalk; spt, subpallial telencephalon; vt, ventral thalamus; pvh, posterior-ventral hypothalamus (infundibulum; presumptive neurohypophysis).

hypothalamus is thought to correspond to the presumptive infundibulum of higher vertebrates, which gives rise to the neurohypophysis (Fürthauer et al., 2001; Mathieu et al., 2002). It is in close contact with the adenohypophyseal cells, which at 26 hpf are located in a horseshoe-like pattern around the anterior and lateral borders of the *fgf3* expression domain (Fig. 3J,M). During further development, the lateral-posterior cells of the adenohypophyseal anlage converge to the midline (Nica et al., 2004) and become located underneath the *fgf3*-expressing cells of the presumptive infundibulum (Fig. 3N,O). By contrast, the anteriormost cells of the adenohypophysis, as characterized by the expression of *prolactin*, are in some distance from the *fgf3*-positive cells (Fig. 3K).

Comparative in-situ hybridizations with *fgf8* further reveal that the *fgf3*-positive cells of the infundibular region lack *fgf8* expression (compare Fig. 3G with 3H), which instead is weakly expressed in parts of the adenohypophyseal anlage itself and in posteriormost regions of the ventral diencephalon (Fig. 3H). Another site of unique *fgf3* expression is the posterior pharyngeal endoderm (Fig. 3G,H), explaining the gill arch defects of *fgf3* mutants (see above).

Fgf3 is required for the early steps of adenohypophyseal specification

As a first step to characterize the adenohypophyseal defects of *fgf3* mutants, we carried out in-situ hybridizations at various stages of development. Placodal ectoderm starts to be specified toward the end of gastrulation, indicated by the expression of *eya1*, *dlx3* or *pitx3*. All of them are expressed throughout the entire placodal field, while marker genes specific for the different placodes along the anterior–posterior axis of the embryo (adenohypophysis, olfactory, lense, otic etc.) only come up later. At tailbud stage (10 hpf), *fgf3* mutants display normal expression of *eya1* (Fig. 4A,B), *dlx3* and *pitx3* (data not shown), indicating that Fgf3 is not required for the earliest steps of general placodal specification. Similar unaltered expression patterns were found in *fgf3* and *fgf8* (*ace*) (Reifers et al., 1998) double mutants, and in embryos treated with the Fgf receptor inhibitor SU5402 from mid- through late-gastrula stages (Mohammadi et al., 1997) (data not shown), indicating that early placodal development is independent of Fgf signaling in general.

The first currently known adenohypophysis-specific zebrafish marker genes [*pit1* (Nica et al., 2004); *lim3* (Glasgow et al., 1997)] start to be expressed around the 19-somite stage (18.5 hpf), slightly after the initiation of *fgf3* expression in the infundibular region (see above). In *fgf3* mutants, expression of *pit1* and *lim3* fails to be initiated (Fig. 4C-F for *pit1* at 19 hpf, *lim3* at 24 hpf). Similarly, no transcripts of adenohypophyseal hormones can be detected at any stage (Fig. 4K,L for *pomc* at 72 hpf, and data not shown).

The infundibular region itself appears to be less affected by the *fgf3* mutations. Infundibular cells of mutant embryos lack expression of the Fgf target gene and autocrine feedback antagonist *sprouty4* (*spry4*) (Fig. 4I,J) (Fürthauer et al., 2001). However, *fgf3* mutants display normal infundibular expression of *fgf3* at 36 hpf (Fig. 2E,F) and later (48 hpf, 72 hpf, data not shown), indicating that infundibular cells are maintained, and that in contrast to Fgf8 (Reifers et al., 1998; Heisenberg et al., 1999), Fgf3 is not required for the maintenance of its own expression.

Like the infundibulum, which is part of the tuberal, posterior-ventral hypothalamus, other regions of the ventral diencephalon appear to develop independently of Fgf3, too. This is indicated by the unaltered expression of *shh* (Fig. 4G,H), a marker for the

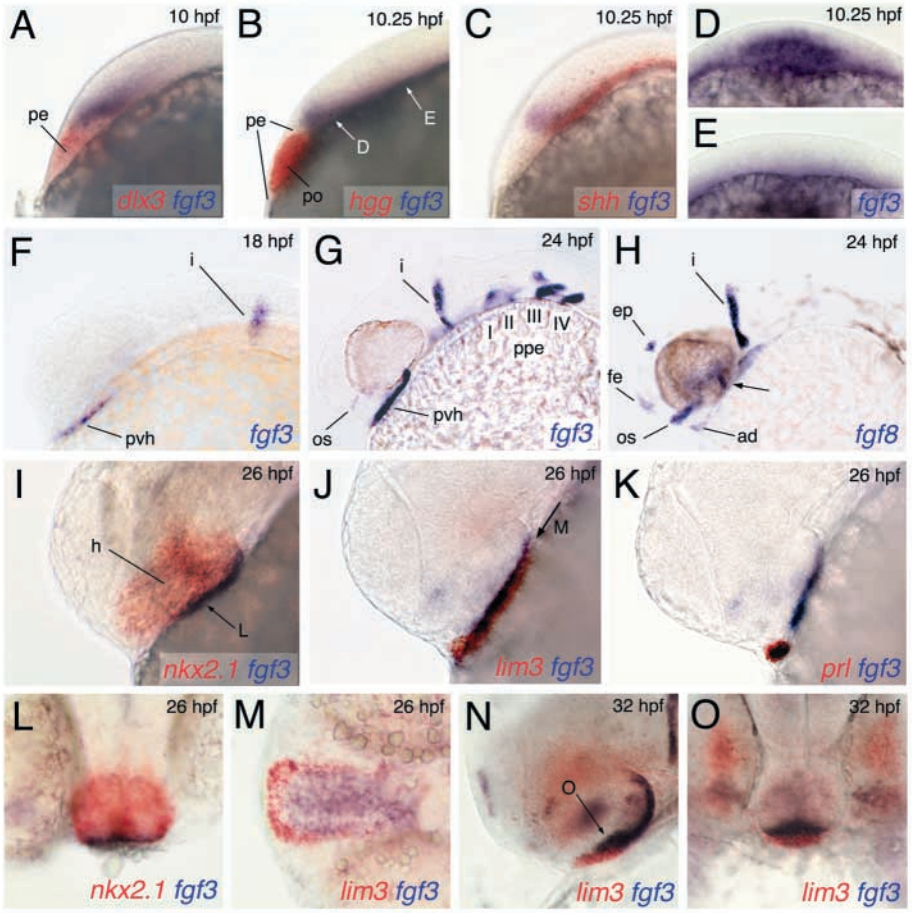

Fig. 3. The adenohypophyseal anlage is faced by *fgf3*-expressing telencephalic cells early, and ventral diencephalic cells later. Probes used for in-situ hybridizations are indicated in the corresponding colors in the lower right corners, ages of embryos in the upper right corners. (A-C,F-K,N) Lateral views on head region. (D,E,L,O) Transverse optical sections. (N) Sagittal section. White arrows in B indicate levels of optical cross sections shown in (D,E). Numbers in G mark pharyngeal arches (see Fig. 2). Arrow in H indicates *fgf8*-positive cells in posteriormost regions of the posterior-ventral hypothalamus. Arrow in I indicates level of optical cross section shown in L, arrow in J indicates sagittal section shown in M, arrow in N cross section shown in O. ad, adenohypophysis; ep, epiphysis; fe, facial ectoderm; h, hypothalamus; i, isthmus; os, optic stalk; pe, placodal ectoderm; po, polster; pvh, posterior-ventral hypothalamus; ppe, pharyngeal pouch endoderm.

anterior-dorsal hypothalamus (Mathieu et al., 2002), and by the normal expression of *pomc* in endorphin-synthesizing hypothalamic neurons of mutant embryos (Fig. 4K,L).

Adenohypophyseal development is driven by Fgf3 from the diencephalon

As described above, adenohypophyseal cells are exposed to Fgf3 signals from different sources (telencephalon, diencephalon) and at different stages of development (end of gastrulation, midsegmentation) (Fig. 3). To determine the source of Fgf3 required for adenohypophyseal development, we generated mosaic embryos, transplanting presumptive telencephalic or diencephalic cells from early gastrula wild-type donor embryos into the same regions of *fgf3* mutant recipients (Fig. 5B). We found that wild-type cells in the ventral region of the diencephalon rescued *lim3* expression in adjacent adenohypophyseal cells of *fgf3* mutants (Fig. 5E,F; *n*=9). By contrast, even largest clones of wild-type cells in the telencephalon of *fgf3* mutants failed to rescue *lim3* expression (Fig. 5G,H; *n*=8). This indicates that it is Fgf3 from the ventral diencephalons that is required in a non-cell autonomous fashion to instruct adenohypophyseal specification in the underlying placodal ectoderm.

Fgf signaling governing adenohypophysis development is required during midsegmentation stages

To narrow down the time window during which Fgf3 from the forebrain is required for adenohypophysis development, two kinds of experiments were carried out. To block Fgf signaling in a temporally controlled fashion, we treated wild-type embryos at various stages with the Fgf receptor inhibitor SU5402 (Mohammadi et al., 1997). Embryos treated during midsegmentation stages (18-22 hpf) show a complete loss of *lim3*, *pomc* and *prl* expression at 34 hpf, while head morphology appears normal (Fig. 6E-H, and data not shown) (284/286 embryos without adenohypophyseal marker gene expression; 6 independent experiments). In comparison, SU5402 treatment during gastrulation and early segmentation stages (8-12 hpf) led to milder adenohypophyseal defects (66/138 embryos without, 72/138 with, reduced adenohypophyseal marker gene expression; data not shown), although such embryos display strong brain defects (data not shown) (cf. Walshe et al., 2003a). In sum, the data show that Fgf signaling during midsegmentation stages is absolutely required for adenohypophyseal development, while the importance of earlier Fgf signaling is less clear (see Discussion).

A requirement of Fgf signaling during midsegmentation stages is also revealed by bead implantation studies. When implanted into the diencephalon of mutant embryos between the 18- and 20-somite stages (19 hpf), Fgf3-loaded beads led to a significant rescue of adenohypophyseal *lim3* expression at 26 hpf (Fig. 6B,C) (9/9; 2 independent experiments). By contrast, BSA-loaded control beads had no effect (Fig. 6D) (0/5).

In sum, these experiments indicate that adenohypophysis development depends on Fgf3 during stages when it is normally expressed in the presumptive infundibular region.

Shh cannot rescue adenohypophyseal development but can induce ectopic pituitary cells in other placodal regions of *fgf3* mutants

In addition to Fgfs, the diencephalon is known to be the source

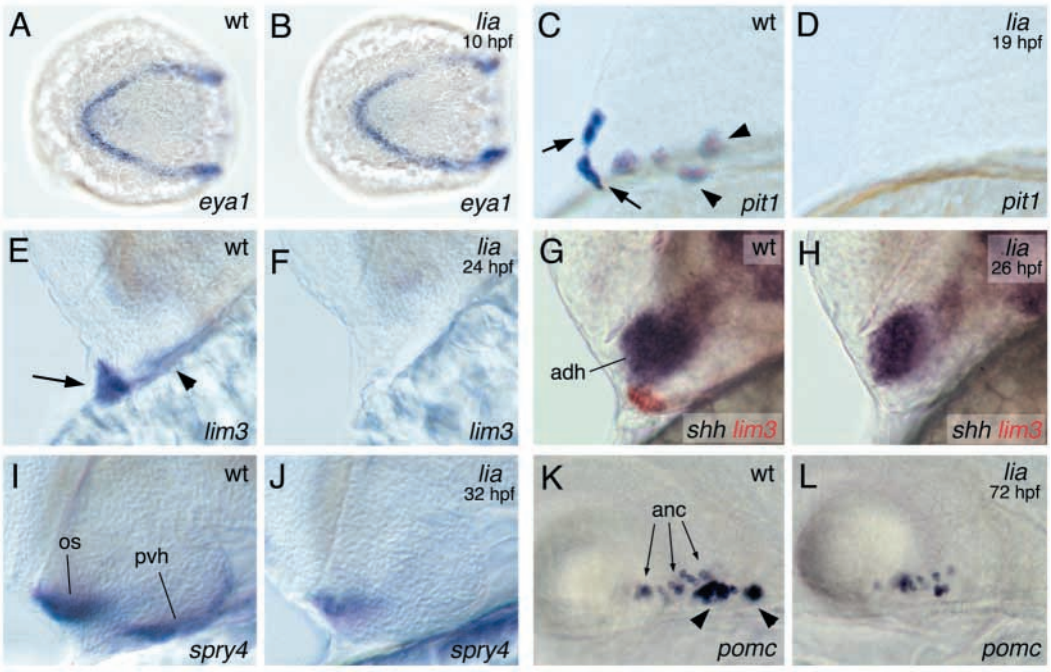

Fig. 4. *fgf3* mutants fail to initiate the expression of early pituitary-specifying genes, whereas the hypothalamus develops normally. Probes used for in situ-hybridizations are indicated in the lower right corners. (A,C,E,G,I,K) Wild-type siblings (wt). (B,D,F,H,J,L) *fgf3* mutants (*lia*), with age of embryos indicated in the upper right corners. (A,B) Tailbud stage, animal views, dorsal to the right; embryos were genotyped after photography. (C-L) Lateral views on heads. Arrows in (C,E) indicate expression in anterior domain, arrowheads expression in lateral posterior domains of adenohypophyseal anlage [compare with Fig. 3M and Nica et al. (Nica et al., 2004)]. Arrowheads in (K) indicate the two adenohypophyseal *pomc* expression domains. anc, endorphin-synthesizing arcuate nuclei cells of hypothalamus; fe, facial ectoderm; adh, anterior-dorsal hypothalamus; i, isthmus; os, optic stalk; pvh, posterior-ventral hypothalamus.

of other crucial signals driving adenohypophysis development. One of the identified diencephalic signals governing pituitary induction, patterning and growth in mouse and zebrafish is Sonic Hedgehog (Shh) from the anterior-dorsal hypothalamus (Treier et al., 2001; Herzog et al., 2003; Sbrogna et al., 2003) (see Fig. 4G). In light of results obtained for other developmental processes such as limb/pectoral fin development, proposing a role of Fgf signaling to activate *shh* expression (Fischer et al., 2003), we wanted to investigate whether neurohypophyseal Fgf3 might regulate

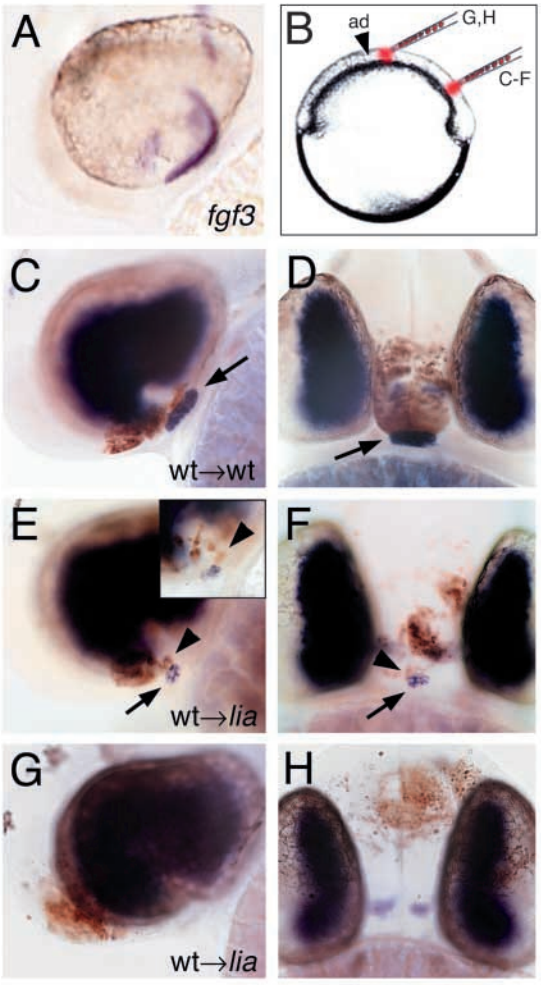

Fig. 5. Fgf3 signaling from the diencephalon, but not the telencephalon, is sufficient for adenohypophyseal development. (A,C-H) Embryos at 32 hpf, lateral views (A,C,F,G), or frontal views (D,F,H), on head regions. (A) Embryo stained for *fgf3* transcripts. Note the fissure of the eye vesicle as a reference point for the anterior border of the infundibular *fgf3* expression domain. (B) Cartoon showing the transplantation sites at shield stages. Consistent with results obtained in fate-mapping experiments (Woo and Fraser, 1995; Varga et al., 1999; Mathieu et al., 2002), telencephalic chimeras as shown in G,H were obtained by transplanting cells from/to the animal pole, diencephalic chimeras as shown in C-F by transplanting cells from/to dorsal regions anterior/animal of the shield. Cells of the adenohypophysis (ad) are supposed to derive from region indicated by arrowhead. (C-H) Chimeras, in-situ hybridized for *lim3* transcripts in blue, and with transplanted wild-type cells in brown. Out-of-focus bilateral *lim3* domains in D,F,H represent hindbrain motoneurons (Glasgow et al., 1997). (C,D) Wild-type recipients with wild-type donor cells in the diencephalon, displaying normal adenohypophyseal *lim3* expression (indicated by arrows). (E,F) *fgf3* mutant recipients with infundibular wild-type cells (indicated by arrowheads) and adjacent rescued adenohypophyseal *lim3* expression (indicated by arrows). Inset in E shows second rescued embryo. (G,H) *fgf3* mutant recipient with many wild-type cells in the telencephalon, still lacking adenohypophyseal *lim3* expression.

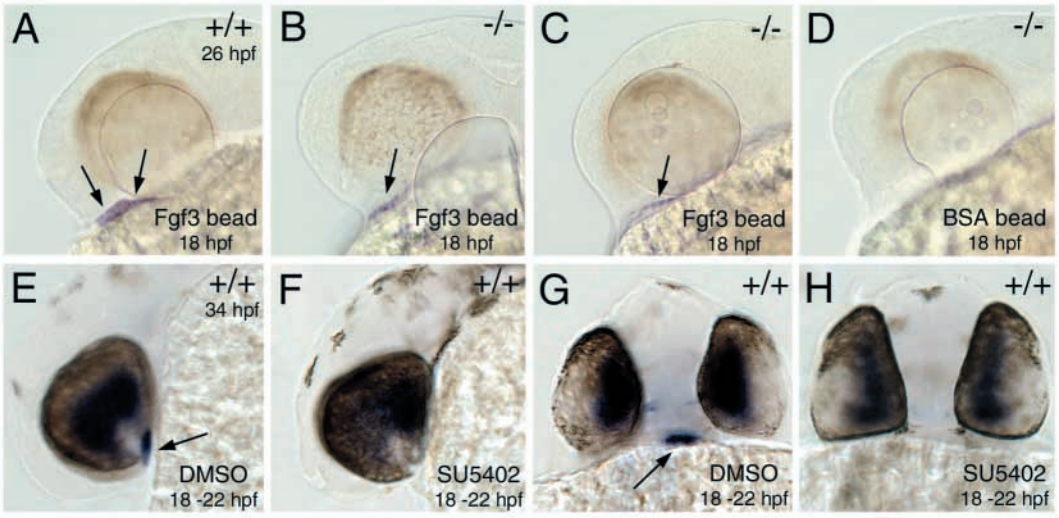

Fig. 6. Fgf signaling governing adenohypophysis development is required during midsegmentation stages. All panels show embryos after *lim3* in-situ hybridization. Adenohypophyseal *lim3* staining in (A-C,E,G) is indicated by arrows. (A-D) Bead implantations, performed at 18 hpf. Panels show lateral views on heads of embryos at 26 hpf. Embryos were genotyped after photography. (A) Implant of Fgf3 bead into wild-type sibling embryo. (B,C) Implant of Fgf3 beads into mutant embryos, leading to partial rescue of adenohypophyseal *lim3* expression; note bead position far from the telencephalon in (B). (D) Implant of BSA bead into mutant embryo. (E-H) SU5402 treatments. (E,F) Lateral views, (G,H) frontal views on heads of embryos at 34 hpf. Incubation of embryo in 20 μM SU5402 from 18-22 hpf leads to complete loss of adenohypophyseal *lim3* expression, while control embryo treated with DMSO is unaffected.

adenohypophyseal development via Shh. For this purpose, *fgf3* mutant embryos were injected with *shh* mRNA. However, *shh*-injected *fgf3* mutants still lacked endogenous *pomc* and *prl* expression in the adenohypophyseal domain (Fig. 7B), indicating that Shh cannot compensate for the loss of Fgf3 and suggesting that Fgf3 acts in parallel to, rather than upstream of, Shh.

By contrast to the adenohypophysis itself, injected *shh* mRNA has a striking effect on adenohypophyseal gene expression in ectopic positions. In wild-type embryos, forced *shh* expression leads to ectopic *pomc* and *prl* expression in more lateral/posterior regions of the placodal ectoderm (Fig. 7A,C). These cells most probably represent trans-fated cells of the lense and otic placodes (Herzog et al., 2003) (note segmented pattern of *prl* expression in Fig. 7C). A similar ectopic induction of *pomc* and *prl* expression was also obtained in *fgf3* mutants (Fig. 7B), indicating that in such ectopic locations, adenohypophyseal cells can specify independently of Fgf3 activity. They appear to require other Fgfs that act instead of, or in addition to, Fgf3. This is indicated by the effect of the Fgf receptor inhibitor SU5402, which, by contrast to *fgf3* mutations, blocks both the endogenous and the Shh-induced ectopic *prl* expression to similar extents (Fig. 7D).

Unspecified adenohypophyseal cells of *fgf3* mutants die by subsequent apoptosis

In Hedgehog signaling pathway mutants, the adenohypophysis is trans-fated to lens material (Kondoh et al., 2000; Varga et al., 2001). Several experiments were carried out to investigate the fate of non-specifying adenohypophyseal cells in *fgf3* mutant embryos. At 24 hpf, the ANR region of mutant embryos appeared morphologically normal, despite the lack of *lim3* expression (Fig. 4E,F). Using Nomarski optics, the adenohypophysis of wild-type embryos became visible as a distinct organ at approximately 25 hpf (Fig. 8A). An organ of similar size and shape, and at the same position, was also present in *fgf3* mutants at 25 hpf (Fig. 8B). However, by 28 hpf

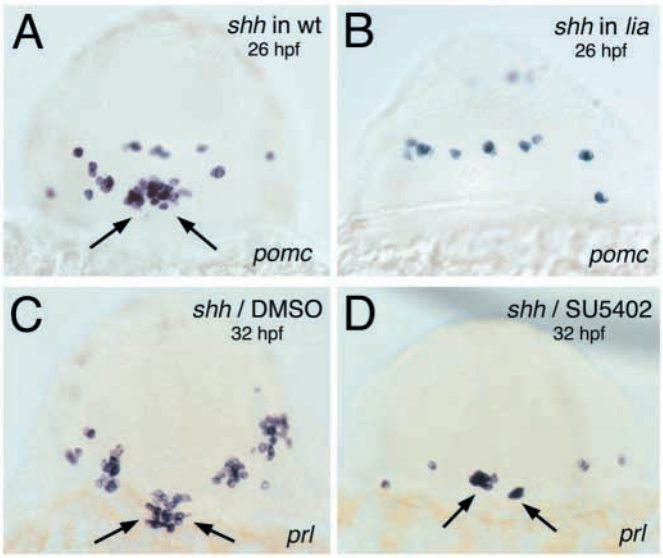

Fig. 7. Shh cannot rescue the normal adenohypophysis of *fgf3* mutants, but can induce ectopic adenohypophyseal cell specification in an Fgf-dependent manner. All panels show embryos injected with *shh* mRNA at the 1-cell stage, frontal views on heads. Probes used for in-situ hybridizations are indicated in the lower right corners, ages of embryos, and genotype or further treatment in the upper right corners. (A,C) Wild-type controls; the regular *pomc* or *prl* expression domains are indicated by arrows. (B) *fgf3* mutant, displaying *pomc*-positive cells in ectopic positions, whereas the regular region of the adenohypophyseal anlage remains *pomc*-negative embryo. (D) Moderately affected embryo treated with 12 μM SU54302 from 15-32 hpf, displaying a partial loss of both endogenous and ectopic *prl*-positive cells. The effect on ectopic *prl* expression was weaker after SU5402 treatment from 18-22 hpf (data not shown), suggesting that Fgf signaling promoting adenohypophyseal specification in ectopic positions occurs over a longer time period than that by Fgf3 from the infundibular region required for the regular adenohypophysis (compare with Fig. 6E-H).

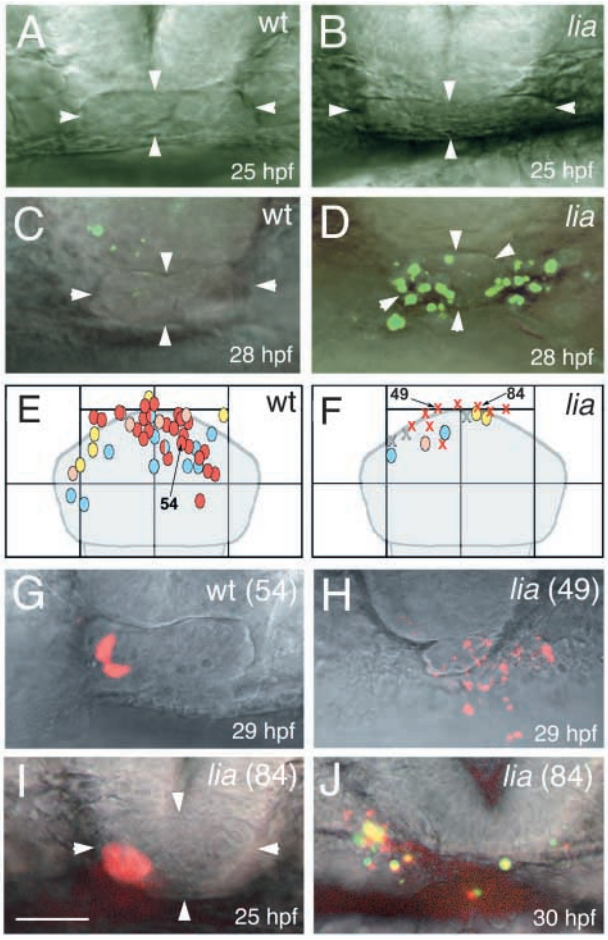

Fig. 8. Non-specifying adenohypophyseal cells of *fgf3* mutants undergo apoptosis. (A-D,I,J) Nomarski images, (G,H) confocal images; frontal views onto the anterior border of the head, superimposed with fluorescent images of Acridine Orange stainings in green (C,D,J), or rhodamine cell labelings in red (G-J). All images are at same magnification; scale bar shown in (I) = 25 μm. In A-D,I, borders of the adenohypophysis are indicated with white arrowheads. All embryos were genotyped after evaluation and photography. (A) Nomarski images at 25 hpf; wild-type sibling; (B) *fgf3* mutant, displaying a normal-sized adenohypophysis. For better contrast, images are not superimposed with Acridine Orange stainings, which showed no positive cells for wild-type (A), but few positive cells for mutant (B). (C,D) Acridine Orange stainings at 28 hpf; (C) wild-type sibling; (D) *fgf3* mutant. (E,F) Summary of single cell-tracing experiments: cartoons showing the position of single cells from the anterior neural ridge region labeled at the tailbud stage, relative to mesodermal polster outlined in gray, which served as a landmark for the injections. A square corresponds to 50 μm × 50 μm. The fate of each cell is indicated by shape and color. Circles mark cells whose daughter cells were alive 28-30 hpf, crosses indicate cells that died during the course of the analysis, resulting in labeled cell debris only. Red circles mark adenohypophyseal clones, blue circles olfactory epithelium clones, yellow circles facial ectoderm clones, and salmon circles clones ending up in the head mesenchyme. Mixed clones with descendants in two different tissues are indicated with two-colored circles. Numbers and arrows mark cells with descendants shown in G-J. (E) Cells from wild-type siblings; (F) cells from *fgf3* mutants. In F, red crosses represent clones with debris within and outside the shrunken adenohypophysis. Gray crosses are clones with debris outside the adenohypophysis only, which had not been investigated at 24 hpf. Therefore, their initial tissue belongings cannot be stated; however, they most likely derive from adenohypophyseal cells that had died early. (G) Descendants of wild-type cell 54 at 29 hpf. (H) Cell debris deriving from mutant cell 49. (I,J) Time course analyses of mutant cell 84. (I) 25 hpf; (H) same embryo at 30 hpf, counterstained with Acridine Orange.

and 29 hpf, the size of the adenohypophysis in mutants had become progressively smaller (Fig. 8D,H), while in wild-type siblings, it was similar to the size at 25 hpf (Fig. 8C,G).

To investigate the reasons for this regression of the organ in *fgf3* mutants, we performed Acridine Orange stainings to detect apoptotic cells. At the 20-somite stage (19 hpf; 4 genotyped mutants) and at 24 hpf (5 genotyped mutants), apoptosis rates in the ANR region of mutant and wild-type sibling embryos were low and undistinguishable (data not shown). However, at 28 hpf, *fgf3* mutants showed significantly more apoptotic cells in and around the shrunken adenohypophysis (Fig. 8D; 5 genotyped mutants) than wild-type siblings (Fig. 8C). The Acridine Orange signals outside the adenohypophysis could stem from either apoptotic cells of adjacent tissues or adenohypophyseal cells with debris extruded from the organ. To distinguish between these possibilities, we performed cell-tracing experiments, following the fate of single cells from the ANR region after labeling at tailbud stage (Fig. 8E,F). Live cells that contribute to olfactory epithelium, facial ectoderm and head mesenchyme were labeled with similar frequencies in mutant and wild-type sibling embryos (Fig. 8E,F). However, while most of the labeled cells in wild-type embryos gave rise to the adenohypophysis (Fig. 8E,G), not a single live adenohypophyseal cell was obtained in mutants at 28-30 hpf. Instead, cell debris was found in and around the disintegrating organ (Fig. 8F,H). Time course analyses showed that this debris – even that outside the pituitary gland – stems from adenohypophyseal cells that appear alive at 25 hpf (Fig. 8I) but become apoptotic and Acridine Orange-positive within the next hours (Fig. 8J). Together, these data indicate that in the absence of Fgf3 signaling, adenohypophyseal cells undergo apoptosis, while other cell types coming from the ANR region develop normally. Adenohypophyseal cell death starts a few hours after the failed transcriptional activation of *lim3* and *pit1*, pointing to a possible correlation between cell specification and cell survival processes.

Discussion

Fgf3 and Fgf10 in mouse and zebrafish

The different members of the family of Fgf ligands can be subgrouped according to sequence similarities and receptor specificities (Ornitz et al., 1996; Powers et al., 2000). Fgf3 mainly binds to the IIIb isoform of Fgf receptor 2 (Fgfr2IIIB), as does Fgf10. In mouse, mutants lacking Fgf10 (Ohuchi et al., 2000) or Fgfr2IIIb (Min et al., 1998; Sekine et al., 1999; De Moerlooze et al., 2000) display very similar defects during the formation of numerous organs, including the pituitary, suggesting that Fgf10 is the major ligand of Fgfr2IIIb. In comparison, *Fgf3* deficient mice have rather subtle and more restricted defects during the late stages of tail and inner ear development (Mansour et al., 1993). Comparing the

phenotypes of mutants in mouse and zebrafish, it appears that the functions of Fgf3 and Fgf10 have partly interchanged. During pituitary development, zebrafish Fgf3 seems to play the same role as mouse Fgf10. This is in contrast to pectoral fin/limb bud development, during which Fgf10 appears to be at play both in mouse and zebrafish (Min et al., 1998; Sekine et al., 1999; Ng et al., 2002).

Early and late roles of Fgf signaling during adenohypophyseal development?

The mouse infundibulum expresses at least three different Fgfs, *Fgf10* of the Fgfr2IIIb-binding subgroup, and *Fgf8* and *Fgf18* of the IIIc group (Maruoka et al., 1998). The requirement of Fgf8 signaling for adenohypophyseal development has not been addressed as yet, due to early embryonic lethality of *Fgf8* mutant embryos (Meyers et al., 1998; Sun et al., 1999). However, *Fgf10* mutants are viable until birth, and their phenotype suggests an essential role of Fgf10 affecting all adenohypophyseal cell types before definitive pouch formation (E10) (Ohuchi et al., 2000). Furthermore, results obtained upon treatment of E10 pouch explants with the Fgf receptor inhibitor SU5402 suggest an additional later role of Fgf signaling to pattern the definitive pouch along its dorsoventral axis (Norlin et al., 2000). In zebrafish, our expression pattern analyses even suggest a third, much earlier, phase of Fgf signaling, which might occur during late gastrulation stages, when adenohypophyseal progenitor cells are located at the ANR and in close proximity to *fgf3*- and *fgf8*-expressing cells of the presumptive telencephalon (Fig. 3). Our rescue experiments via transplantation of wild-type cells or implantation of Fgf3 beads, as well as our experiments with temporally controlled blockage of Fgf signaling by SU5402, indicate that the later Fgf3 from the ventral diencephalon is absolutely necessary for adenohypophysis formation. Whether the earlier Fgf3 from the telencephalon is required, too, is less clear. The rescue of *lim3* expression by diencephalic wild-type cells or late Fgf3 bead implants is only partial, never yielding *lim3* expression in the entire adenohypophyseal domain. Similarly, early SU5402 treatment of embryos during gastrulation and early segmentation stages also leads to a strong reduction of adenohypophyseal marker gene expression, which, however, could be a secondary consequence of the effect of SU5402 on hypothalamus development. In sum, we can neither prove, nor rule out, an involvement of early telencephalic Fgf3 signaling on adenohypophysis development.

In addition to this general role affecting all pituitary cell types, Fgf3 signaling might also have a cell type-discriminating function to pattern the zebrafish adenohypophysis, similar to the proposed morphogenetic role of Fgf8 in mouse. As in mouse, the different cell types of the zebrafish adenohypophysis display a differential distribution along the dorsoventral axis of the anlage (Liu et al., 2003b; Nica et al., 2004), with dorsal cells being closer to the infundibulum than ventral cells. In addition, the zebrafish adenohypophysis is patterned along its antero-posterior axis (Herzog et al., 2003), with posterior cell types being closer to the infundibular Fgf3 domain than anterior cells. In conclusion, different adenohypophyseal cell types might indeed be exposed to different doses of Fgf3 signals. It is currently unclear whether this has any effects on the patterning of the adenohypophysis. This question cannot be addressed via regular analyses of *fgf3* mutants, due to the earlier requirement of Fgf3 signaling for all adenohypophyseal cell types. Approaches allowing temporally controlled blockage of Fgf signaling have to be entertained, such as late applications of the inhibitor SU5402.

The subsequent effects of Fgf3 signaling on cell specification and cell survival

During mouse adenohypophysis development, Fgf signaling is supposed to have diverse effects on target cells, regulating organ morphogenesis and patterning, cell proliferation, cell survival and cell specification (see Introduction). Here, we investigated how these different effects might be correlated, studying the time course with which the different phenotypic aspects arise during adenohypophyseal development of *fgf3* mutant zebrafish. First defects are concerned with early adenohypophysis-specific specification steps. While the general specification of the placodal ectoderm at the interphase of neural and non-neural ectoderm (10-12 hpf) (for a review, see Baker and Bronner-Fraser, 2001) occurs normally in mutant embryos, later (18.5 hpf) they fail to initiate expression of the adenohypophyseal-specific marker genes *lim3* and *pit1* in the ANR, the anteriormost region of the placodal domain. This, however, neither affects the proliferation of adenohypophyseal progenitor cells nor further pituitary morphogenesis. At 25 hpf, *fgf3* mutants display a pituitary gland of relatively normal size and shape. Also, we failed to detect any differences in BrdU incorporation studies (W.H. and M.H., unpublished data). However, we found dramatic apoptosis of adenohypophyseal cells after organ formation, starting at 25 hpf, and leading to a complete loss of the organ within 5 hours.

In conclusion, it appears that Fgf3 signaling primarily induces the activation of genes involved in early steps of adenohypophyseal specification, subsequently affecting cell survival. Pituitary morphogenesis and growth is affected even later, most probably as a consequence of the death of adenohypophyseal cells. However, it still remains largely unclear how Fgf3-induced cell specification and cell survival processes are correlated. *pit1* and *lim3* might be direct target genes of Fgf3 signaling, as their expression appears to be initiated shortly after the onset of *fgf3* expression in the presumptive neurohypophysis (18 hpf versus 18.5 hpf). This would be consistent with the proposed role of Fgf8 in activating *Lhx3* expression in mouse (Takuma et al., 1998; Ericson et al., 1998). In mouse, Pit-1 and Lhx3 have been shown to be directly involved in the transcriptional activation of hormone-encoding genes (Anderson and Rosenfeld, 2001; Lamolet et al., 2001; Liu et al., 2001), explaining why zebrafish *fgf3* mutants fail to initiate *prl* and *pomc* expression at 24 hpf. It remains unclear whether the subsequent death of adenohypophyseal cells between 25 hpf and 30 hpf is a default consequence of their failed specification/differentiation, or whether Fgf3 activates the transcription of additional genes, particularly regulating cell survival.

Differential effects of Fgf and Shh signaling

In midsegmentation zebrafish embryos, such survival factors appear also to be present in other tissues, where they are generated in response to other or additional Fgf signals. This is indicated by our observation that Shh can induce the formation of viable lactotropes and corticotropes in ectopic

placodal locations in an Fgf3-independent, but SU5402-sensitive, manner. According to their position, the intermediate domains of ectopic *prl*-positive cells in *shh*-injected embryos most probably represent trans-fated lense precursor cells, which might survive due to the redundant function of Fgf3 and Fgf8 from the optic stalk. In *shh*-injected embryos, this optic stalk is laterally enlarged (Macdonald et al., 1995), and therefore close to the trans-fated placodal lense precursor cells.

The *shh* overexpression studies further show that Fgf3 does not simply act via an activation of *shh*, as Shh is not capable of rescuing pituitary cell types in the adenohypophyseal region itself. Rather, Fgf3 and Shh appear to act in parallel and to have rather distinct effects. Thus, ectopic Shh can induce the expression of adenohypophyseal genes in ectopic locations, whereas Fgf3 cannot (Fig. 7; W.H. and M.H., unpublished observations). Furthermore, Shh has mitogenic activity, indicated by the reduced growth of the adenohypophysis in *shh* mutants without any sign of increased cell death, whereas the adenohypophysis of *fgf3* mutants shrinks due to loss of cells by apoptosis.

We are very grateful to the other members of the Freiburg screening group (M. Schorpp, D. Diekhoff, T. Franz, M. Leicht, E. Nold, T. Nolting, C. Riegger, W. Wiest), and of the Tuebingen screen consortium (MPI for Developmental Biology: F. van Bebber, E. Busch-Nentwich, R. Dahm, H.-G. Frohnhöfer, H. Geiger, D. Gilmour, S. Holley, J. Hooge, D. Jülich, H. Knaut, F. Maderspacher, H.-M. Maischein, C. Neumann, T. Nicolson, C. Nüsslein-Volhard, U. Schönberger, C. Seiler, C. Söllner, M. Sonawane, A. Wehner, C. Weiler; Exelixis Germany GmbH: P. Erker, H. Habeck, U. Hagner, C. Hennen, E. Kaps, A. Kirchner, T. Koblitzek, U. Langheinrich, C. Loeschke, C. Metzger, R. Nordin, J. Odenthal, M. Pezzuti, K. Schlombs, J. deSatana-Stamm, T. Trowe, G. Vacun, B. Walderich, A. Walker, C. Weiler) for carrying out the screen during which the *lia* alleles were isolated. We are also very grateful to Filippo Del Bene and Jochen Wittbrodt for teaching us the bead implantation technique. M.H. thanks Thomas Boehm, Z.M.V. thanks Wolfgang Driever, and H.H.R. thanks Christiane Nüsslein-Volhard for support and discussions. We are grateful for the help and technical support from Roland Nitschke and the Life Imaging Facility of the SFB 592 (Z2) during confocal microscopy. Many thanks also to Michael Brand (*ace*, *fgf8*, *krox20*), Chi-Yao Chang (*gh*), Igor Dawid (*lim3*), Mark Ekker (*dlx2*, *dlx3*), Christine Petit (*eya1*), Corinne Houart (*emx1*), Phil Ingham (*shh*), Klaus Rohr (*nkx2.1*), and Bernard and Christine Thisse (*fgf3*, *hgg*, *spry4*) for mutants and plasmids. Work in the laboratories of M.H. and H.H.R. was supported by the Max-Planck Society, work in Z.M.V.'s laboratory by the Sonderforschungsbereich SFB 592 (A5).

References

Akimenko, M.-A., Ekker, M., Wegner, J., Lin, W. and Westerfield, M. (1994). Combinatorial expression of three zebrafish genes related to *distal-less*: part of a homeobox gene code for the head. *J. Neurosci.* **16**, 3475-3486.

Anderson, B. and Rosenfeld, M. G. (2001). POU domain factors in the neuroendocrine system: lessons from developmental biology provide insights into human disease. *Endocrinol. Rev.* **22**, 2-35.

Baker, C. V. H. and Bronner-Fraser, M. (2001). Vertebrate cranial placodes I: embryonic induction. *Dev. Biol.* **232**, 1-61.

Burgess, R., Lunyak, V. and Rosenfeld, M. G. (2002). Signaling and transcriptional control of pituitary development. *Curr. Opin. Genet. Dev.* **12**, 534-539.

David, N. B., Saint-Etienne, L., Tsang, M., Schilling, T. F. and Rosa, F. M. (2002). Requirement for endoderm and FGF3 in ventral skeleton formation. *Development* **129**, 4457-4468.

De Moerlooze, L., Spencer-Dene, B., Revest, J.-M., Hajihosseini, M., Rosewell, I. and Dickson, C. (2000). An important role for the IIIb isoform of fibroblast growth factor 2 (FGFR2) in mesenchymal-epithelial signaling during mouse organogenesis. *Development* **127**, 483-492.

Ericson, J., Norlin, S., Jessell, T. M. and Edlund, T. (1998). Integrated FGF and BMP signaling controls the progression of progenitor cell differentiation and the emergence of pattern in the embryonic anterior pituitary. *Development* **125**, 1005-1015.

Fischer, S., Draper, B. W. and Neumann, C. J. (2003). The zebrafish *fgf24* mutant identifies an additional level of Fgf signaling involved in vertebrate forelimb initiation. *Development* **130**, 3515-3524.

Fürthauer, M., Reifers, F., Brand, M., Thisse, B. and Thisse, C. (2001). *sprouty4* acts in vivo as a feedback-induced antagonist of FGF signaling in zebrafish. *Development* **128**, 2175-2186.

Fürthauer, M., Thisse, C. and Thisse, B. (1997). A role for FGF-8 in the dorsoventral patterning of the zebrafish gastrula. *Development* **124**, 4253-4264.

Geisler, R. (2002). Mapping and cloning. In *Zebrafish, Practical approach*, vol. 261 (ed. C. Nüsslein-Volhard and R. Dahm), pp. 175-212. Oxford, UK: Oxford University Press.

Glasgow, E., Karavanov, A. A. and Dawid, I. B. (1997). Neuronal and neuroendocrine expression of lim3, a LIM class homeobox gene, is altered in mutant zebrafish with axial signaling defects. *Dev. Biol.* **192**, 405-419.

Hammerschmidt, M., Pelegri, F., Mullins, M. C., Kane, D. A., van Eeden, F. J. M., Granato, M., Brand, M., Furutani-Seiki, M., Haffter, P., Heisenberg, C.-P. et al. (1996). *dino* and *mercedes*, two genes regulating dorsal development in the zebrafish embryo. *Development* **123**, 95-102.

Heisenberg, C.-P., Brennan, C. and Wilson, S. W. (1999). Zebrafish *aussicht* mutant embryos exhibit widespread overexpression of *ace* (*fgf8*) and coincident defects in CNS development. *Development* **126**, 2129-2140.

Herzog, W., Sonntag, C., Walderich, B., Odenthal, J., Maischein, H.-M. and Hammerschmidt, M. (2004). Genetic analysis of adenohypophysis formation in zebrafish. *Mol. Endocrinol.* **18**, 1185-1195.

Herzog, W., Zeng, X., Lele, Z., Sonntag, C., Ting, J.-W., Chang, C.-Y. and Hammerschmidt, M. (2003). Adenohypophysis formation in the zebrafish and its dependence on Sonic Hedgehog. *Dev. Biol.* **254**, 36-49.

Kiefer, P., Strähle, U. and Dickson, C. (1996). The zebrafish *Fgf-3* gene: cDNA sequence, transcript structure and genomic organization. *Gene* **168**, 211-215.

Kondoh, H., Uchikawa, M., Yoda, H., Takeda, H., Furutani-Seiki, M. and Karlstrom, R. O. (2000). Zebrafish mutations in Gli-mediated hedgehog signaling lead to lens transdifferentiation from the adenohypophysis anlage. *Mech. Dev.* **96**, 165-174.

Koshida, S., Shinya, M., Nikaido, M., Ueno, N., Schulte-Merker, S., Kuroiwa, A. and Takeda, H. (2002). Inhibition of BMP activity by the FGF signal promotes posterior neural development in zebrafish. *Dev. Biol.* **244**, 9-20.

Krauss, S., Concordet, J.-P. and Ingham, P. W. (1993). A functionally conserved homolog of the *Drosophila* segment polarity gene *hh* is expressed in tissues with polarizing activity in zebrafish embryos. *Cell* **75**, 1431-1444.

Lamolet, B., Pulichino, A.-M., Lamonerie, T., Gauthier, Y., Brue, T., Enjalbert, A. and Drouin, J. (2001). A pituitary cell-restricted T box factor, Tpit, activates POMC transcription in cooperation with Pitx homeoproteins. *Cell* **104**, 849-859.

Leger, S. and Brand, M. (2002). Fgf8 and Fgf3 are required for zebrafish ear placode induction, maintenance and inner ear patterning. *Mech. Dev.* **119**, 91-108.

Liu, D., Hsin, C., Maves, L., Yan, Y.-L., Morcos, P. A., Postlethwait, J. and Westerfield, M. (2003a). Fgf3 and Fgf8 dependent and independent transcription factors are required for otic placode specification. *Development* **130**, 2213-2224.

Liu, J., Lin, C., Gleiberman, A., Ohgi, K. A., Herman, M. A., Huang, H., Tsai, M. J. and Rosenfeld, M. G. (2001). Tbx19, a tissue-selective regulator of POMC gene expression. *Proc. Natl. Acad. Sci. USA* **98**, 8674-8679.

Macdonald, R., Barth, K. A., Xu, Q., Holder, N., Mikkola, I. and Wilson, S. W. (1995). Midline signalling is required for Pax gene regulation and patterning of the eyes. *Development* **121**, 3267-3278.

Mansour, S. L., Goddard, J. M. and Capecchi, M. R. (1993). Mice homozygous for a targeted disruption of the proto-oncogene *int-2* have developmental defects in the tail and inner ear. *Development* **117**, 13-28.

Maroon, H., Walshe, J., Mahmood, R., Kiefer, P., Dickson, C. and Mason, I. (2002). Fgf3 and Fgf8 are required together for formation of the otic placode and vesicle. *Development* **129**, 2099-2108.

Maruoka, Y., Ohbayashi, N., Hoshikawa, M., Itoh, N., Hogan, B. L. M. and Furuta, Y. (1998). Comparison of the expression of three highly related

genes, Fgf8, Fgf17 and Fgf18, in the mouse embryo. *Mech. Dev.* **74**, 175-177.

Mathieu, J., Barth, A., Rosa, F. M., Wilson, S. W. and Peyriéras, N. (2002). Distinct and cooperative roles of Nodal and Hedgehog signals during hypothalamic development. *Development* **129**, 3055-3065.

Maves, L., Jackman, W. and Kimmel, C. B. (2002). Fgf3 and Fgf8 mediate rhombomere 4 signaling activity in the zebrafish hindbrain. *Development* **129**, 3825-3837.

Meyers, E. N., Lewandoski, M. and Martin, G. R. (1998). An Fgf8 mutant allelic series generated by Cre- and Flp-mediated recombination. *Nat. Genet.* **18**, 136-141.

Min, H., Danilenko, D. M., Scully, S. A., Bolon, B., Ring, B. D., Tarpley, J. E., DeRose, M. and Simonet, W. S. (1998). Fgf-10 is required for both limb and lung development and exhibits striking functional similarity to Drosophila *branchless*. *Genes Dev.* **12**, 3156-3161.

Mohammadi, M., McMahon, G., Sun, L., Tang, C., Hirth, P., Yeh, B. K., Hubbard, S. R. and Schlessinger, J. (1997). Structures of the tyrosine kinase domain of fibroblast growth factor receptor in complex with inhibitors. *Science* **276**, 955-960.

Morita, T., Nitta, H., Kiyama, Y., Mori, H. and Mishina, M. (1995). Differential expression of two zebrafish *emx* homeoprotein mRNAs in the developing brain. *Neurosci. Lett.* **198**, 131-134.

Ng, J. K., Kawakami, Y., Büscher, D., Raya, Á., Itoh, T., Koth, C. M., Esteban, C. R., Rodríguez-León, J., Garrity, D. M., Fishman, M. C. et al. (2002). The limb identity gene *Tbx5* promotes limb initiation by interacting with *Wnt2b* and *Fgf10*. *Development* **129**, 5161-5170.

Nica, G., Herzog, W., Sonntag, C. and Hammerschmidt, M. (2004). Zebrafish *pit1* mutants lack three pituitary cell types and develop severe dwarfism. *Mol. Endocrinol.* **18**, 1196-1209.

Norlin, S., Nordström, U. and Edlund, T. (2000). Fibroblast growth factor signaling in required for the proliferation and patterning of progenitor cells in the developing anterior pituitary. *Mech. Dev.* **96**, 175-182.

Ohuchi, H., Hori, Y., Yamasaki, M., Harada, H., Sekine, K., Kato, S. and Itoh, N. (2000). Fgf10 acts as a major ligand for Fgf receptor 2 IIIb in mouse multi-organ development. *Biochem. Biophys. Res. Com.* **277**, 643-649.

Ornitz, D. M., Xu, J. S., Colvin, J. S., McEwen, D. G., MacArthur, C. A., Coulier, F., Gao, G. X. and Goldfarb, M. (1996). Receptor specificity of the fibroblast growth-factor family. *J. Biol. Chem.* **271**, 15292-15297.

Oxtoby, E. and Jowett, T. (1993). Cloning of the zebrafish Krox-20 (Krx-20) and its expression during hindbrain development. *Nucleic Acids Res.* **21**, 1087-1095.

Phillips, B. T., Bolding, K. and Riley, B. B. (2001). Zebrafish *fgf3* and *fgf8* encode redundant functions required for otic placode induction. *Dev. Biol.* **235**, 351-365.

Powers, C. J., McLeskey, S. W. and Wellstein, A. (2000). Fibroblast growth factors, their receptors and signaling. *Endocr. Relat. Cancer* **7**, 165-197.

Reifers, F., Böhli, H., Walsh, E. C., Crossley, P. H., Stanier, D. Y. R. and Brand, M. (1998). *Fgf8* is mutated in zebrafish acerebellar (ace) mutants and is required for maintenance of midbrain-hindbrain boundary development and somitogenesis. *Development* **125**, 2381-2395.

Rohr, K. B. and Concha, M. L. (2000). Expression of nk2.1a during early development of the thyroid gland in zebrafish. *Mech. Dev.* **95**, 267-270.

Rupp, R. A. W., Snider, L. and Weintraub, H. (1994). *Xenopus* embryos regulate the nuclear localization of XMyoD. *Genes Dev.* **8**, 1311-1323.

Sahly, I., Andermann, P. and Petit, C. (1999). The zebrafish *eya1* gene and its expression during embryogenesis. *Dev. Genes Evol.* **209**, 399-410.

Sbrogna, J. L., Barresi, M. J. F. and Karlstrom, R. O. (2003). Multiple roles for Hedgehog signaling in zebrafish pituitary development. *Dev. Biol.* **254**, 19-35.

Schilling, T. F., Piotrowski, T., Grandel, H., Brand, M., Heisenberg, C. P., Jiang, Y. J., Beuchle, D., Hammerschmidt, M., Kane, D. A., Mullins, M. C. et al. (1996). Jaw and branchial arch mutants in zebrafish I: branchial arches. *Development* **123**, 329-344.

Scully, K. M. and Rosenfeld, M. G. (2002). Pituitary development: regulatory codes in mammalian organogenesis. *Science* **295**, 2231-2235.

Sekine, K., Ohuchi, H., Fujiwara, M., Yamasaki, M., Yoshizawa, T., Sato, T., Yagishita, N., Matsui, D., Koga, Y., Itho, N. et al. (1999). Fgf10 is essential for limb and lung formation. *Nat. Genet.* **21**, 138-141.

Shanmugalingam, S., Houart, C., Picker, A., Reifers, F., Macdonald, R., Barth, A., Griffin, K., Brand, M. and Wilson, S. W. (2000). Ace/Fgf8 is required for forebrain commissure formation and patterning of the telencephalon. *Development* **127**, 2549-2561.

Shinya, M., Koshida, S., Sawada, A., Kuroiwa, A. and Takeda, H. (2001). Fgf signaling through MAPK cascade is required for development of the subpallial telencephalon in zebrafish embryos. *Development* **128**, 4153-4164.

Sun, X., Meyers, E. N., Lewandoski, M. and Martin, G. R. (1999). Targeted disruption of Fgf8 causes failure of cell migration in the gastrulating mouse embryo. *Genes Dev.* **13**, 1834-1846.

Takuma, N., Sheng, H. Z., Furuta, Y., Ward, J. M., Sharma, K., Hogan, B. L. M., Pfaff, S. L., Westphal, H., Kimura, S. and Mahon, K. A. (1998). Formation of Rathke's pouch requires dual induction from the diencephalon. *Development* **125**, 4835-4840.

Thisse, C., Thisse, B., Halpern, M. E. and Postlethwait, J. H. (1994). *goosecoid* expression in neuroectoderm and mesendoderm is disrupted in zebrafish *cyclops* gastrulas. *Dev. Biol.* **164**, 420-429.

Treier, M. and Rosenfeld, M. G. (1996). The hypothalamic-pituitary axis: co-development of two organs. *Curr. Opin. Cell Biol.* **8**, 833-843.

Treier, M., Gleiberman, A. S., O'Connell, S. M., Szeto, D. P., McMahon, J. A., McMahon, A. P. and Rosenfeld, M. G. (1998). Multistep signaling requirements for pituitary organogenesis in vivo. *Genes Dev.* **12**, 1691-1704.

Treier, M., O'Connell, S., Glieberman, A., Price, J., Szeto, D. P., Burgess, R., Chuang, P. T., McMahon, A. P. and Rosenfeld, M. G. (2001). Hedgehog signaling is required for pituitary gland development. *Development* **128**, 377-386.

Varga, Z. M., Wegner, J. and Westerfield, M. (1999). Anterior movement of ventral diencephalic precursors separates the primordial eye field in the neural plate and requires *cyclops*. *Development* **126**, 5533-5546.

Varga, Z. M., Amores, A., Lewis, K. E., Yan, Y. L., Postlethwait, J. H., Eisen, J. S. and Westerfield, M. (2001). Zebrafish smoothened functions in ventral neural tube specification and axon tract formation. *Development* **128**, 3497-3509.

Walshe, J., Maroon, H., McGonnell, I. M., Dickson, C. and Mason, I. (2002). Establishment of hindbrain segmental identity requires signaling by Fgf3 and Fgf8. *Curr. Biol.* **12**, 1117-1123.

Walshe, J. and Mason, I. (2003a). Unique and combinatorial functions of Fgf3 and Fgf8 during zebrafish forebrain development. *Development* **130**, 4337-4349.

Walshe, J. and Mason, I. (2003b). Fgf signaling is required for formation of cartilage in the head. *Dev. Biol.* **264**, 522-536.

Woo, K. and Fraser, S. E. (1995). Order and coherence of the fate map of the zebrafish nervous system. *Development* **121**, 2595-2609.